Fuel savings of a mini-excavator through a hydraulic hybrid displacement controlled system

Rohit Hippalgaonkar[2]

Email: rohit@purdue.edu

Professor Monika Ivantysynova[1,2]

Email: mivantys@purdue.edu

Josh Zimmerman[1]

Email: zimmerjd@purdue.edu
[1] Department of Agricultural and Biological Engineering, Purdue University, 225 S. University St.
[2] School of Mechanical Engineering, Purdue University, 585 Purdue Mall
West Lafayette, IN - 47907, USA.

Abstract

Following system simulations, displacement controlled actuation on a prototype 5-t mini-excavator demonstrated 40% fuel savings in side-by-side testing over the standard mini-excavator for an aggressive truck-loading cycle. Recently, two hydraulic hybrid architectures with DC actuation (including a novel architecture), were investigated in simulation and showed that addition of energy storage capability to the system enables up to 50% engine downsizing and additional fuel savings, without affecting the performance of digging functions. The theoretically optimal power management strategy for the novel architecture predicts 27% fuel savings over the non-hybrid DC architecture. This paper provides an analysis of the optimal control results, and a machine implementable strategy is derived from these. It is observed that atleast one of the pumps connected to the engine shaft, need to be kept at 100% for most of the cycle, implying that the engine needs to be kept at minimum allowable speed, and a high enough throttle.

KEYWORDS: multi-actuator mobile hydraulics, displacement controlled actuation, optimal control, rule-based power management.

1. Introduction

Multi-actuator mobile machines with hydraulic actuation, such as mini-excavators, backhoes and wheel-loaders all have similar system architectures today. These machines typically use one or two large pumps to supply the required power to all actuators. Control valves are used to control the motion of the actuator and to adjust the pump supply pressure to the actuator load utilizing hydraulic resistances. Displacement controlled (DC) actuation, represents a type of throttle-less hydraulic actuation, using one (or multiple) variable displacement pumps to directly control the motion of the hydraulic linear or rotary actuator. No throttling is required because actuators do not share flows Each actuator has its own flow source and pressure is automatically built-up depending on actuator load. DC has been continually investigated at Prof. Ivantysynova's research group since a new circuit for linear actuators with differential cylinders had been introduced by Rahmfeld and Ivantysynova in 1998 /1/.

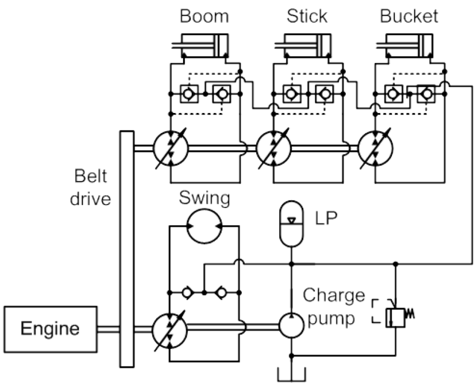

Figure 1: Displacement Controlled Excavator

Figure 1 shows a simplified schematic of the prototype excavator that has been developed. It has one variable displacement pump per working actuator (the auxiliary actuators share a pump with each working actuator, not shown here). Additionally, the pump transmitting power to the swing is directly driven by the engine shaft, while the pumps moving the cylinders are connected through a belt drive, running at a higher speed than the engine. The accumulator in the circuit is not used for energy storage, but is a low pressure (LP) flow source used to account for the unequal flow rates associated with the motion of the single rod cylinders. The logic for balancing these flows is controlled by the pilot operated check valves. This has been implemented on a 5 ton excavator and fuel savings of 40% were measured compared to the standard excavator which uses load sensing hydraulics /2/, on an aggressive truck-loading cycle.

2. Series-Parallel Hydraulic Hybrid DC Excavator

A novel hydraulic hybrid system design for excavators (**Figure 2**) was recently introduced /4/, which is well suited for use with DC actuation. On the DC excavator system, it requires replacement of the original fixed displacement swing motor by a variable displacement swing motor, that is over-center and bi-directional, and is secondary-controlled. Such a system for the swing was first studied by Pederson /3/, and affords energy capture in both directions of motion.

A detailed multi-body dynamic and hydraulic system co-simulation model was developed and used to simulate this architecture on a 5-ton excavator system for an aggressive, truck-loading duty cycle. These results showed that the rated engine power may be up to 50% while meeting performance requirements from the digging functions. The results also showed that as much as 52% fuel savings, over the standard non-hybrid LS excavator system could be achieved by implementing the hybrid DC system and reducing the engine size.

2.1. Sizing Methodology

Assuming the truck-loading cycle to be a limiting case, any energy required at the actuators above the maximum power of the downsized engine (20.5 kW) must be provided for by the high pressure accumulator. The storage pump must be capable of providing the difference between the original rated engine power and the rated power the downsized engine. Additionally, it must be checked that it can supply the maximum power requirement at the swing motor with an empty accumulator. An 18 cc/rev storage pump (identical to the other pumps on the engine shaft) was chosen, together with a 5L accumulator volume. This required a minimum system pressure of 250 bar. Details of the sizing methodology can be found in /4/.

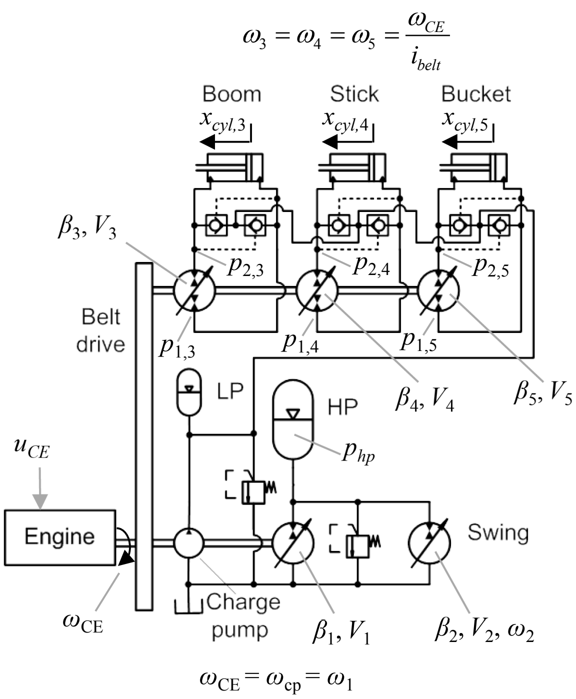

Figure 2: Series-Parallel Hybrid DC Excavator

3. Optimal Power Management for the Hybrid

The potential of further fuel savings through optimal power control have been studied for a given measured operating cycle. Thus, the actuator positions ($\theta_{sw,2}$, $x_{cyl,3}$, $x_{cyl,4}$, $x_{cyl,5}$) and pressures at the pumps ($p_{1,3}$, $p_{2,3}$, $p_{1,4}$, $p_{2,4}$, $p_{1,5}$, $p_{2,5}$) are known beforehand, for every instant of the cycle.

Figure 2 shows that there are six possible degrees of freedom for the hybrid excavator, including the engine throttle (u_{CE}) and the pump displacements (β_1, β_2, β_3, β_4, β_5). Of these, only two are free, since the engine speed n_{CE} and the DC pump displacements β_3, β_4, β_5 are determined by actuator positions ($x_{cyl,3}$, $x_{cyl,4}$, $x_{cyl,5}$) commanded during the cycle, and β_2 is determined by the torque requirements ($M_{sw,2}$) of the swing motor, given the accumulator pressure p_{hp}.

The two free control variables determine the evolution of the 'free' states of the system (p_{hp}, ω_{CE}), while the cycle loads determine the other states of the system (ω_2, $p_{1,3}$, $p_{2,3}$, $p_{1,4}$, $p_{2,4}$, $p_{1,5}$, $p_{2,5}$). Any power management scheme, including the optimal scheme, is a policy for determination of these free control variables while ensuring that cycle requirements on actuators are met.

3.1. State Model

A concise model is explained here. Firstly Eq. (1) describes the dependence of the engine speed on the control variables:

$$\dot{\omega}_{CE} = \frac{1}{J_{CE}}\left[\frac{u_{CE}}{100}\left[M_{WOT}\left(\omega_{CE}\right)+M_f\left(\omega_{CE}\right)\right]-M_f\left(\omega_{CE}\right)-\left[M_1+M_{\text{cp}}+\frac{1}{i_{\text{belt}}}\left(\sum_{\text{i}=3}^{5}M_{\text{i}}\right)\right]\right] \qquad (1)$$

wherein, the first two terms determine the net engine torque output, depending on the engine throttle (u_{CE}), the engine speed (ω_{CE}), the engine's wide-open throttle torque (M_{WOT}) and the engine friction term M_f (which again depends on the engine speed /7/). The third term is the load torque on the engine, which is the sum of the torques applied by the DC pumps, the storage and charge pumps.

Equation (2) relates the pressure build-up in the high pressure accumulator to the controls β_1 and β_2

$$\dot{p}_{\text{hp}} = \frac{1}{C_{\text{H,line}}+C_{\text{accu}}}\left[\left(\frac{\beta_1}{100}\cdot\frac{\omega_1 V_1}{2\pi}-Q_{s,1}\left(\omega_1,p_{hp},\beta_1\right)\right)-\left(\frac{\beta_2}{100}\cdot\frac{\omega_2 V_2}{2\pi}-Q_{s,2}\left(\omega_2,p_{hp},\beta_2\right)\right)\right] \qquad (2)$$

wherein, the first term describes the flow charging the accumulator using the storage pump, while the second term is the flow delivered from the accumulator to the swing motor. The accumulator capacitance changes with pressure build-up, and is given by Eq. (3):

$$C_{\text{accu}} = \frac{V_0}{n}\left(\frac{p_0}{p_{hp}^{\;n+1}}\right)^{1/n} \tag{3}$$

3.2. Dynamic Programming For Series-Parallel Hybrid Excavator

Dynamic programming is a useful tool that determines the optimal control history and optimal state trajectory for a problem, given a set of initial conditions. It is based on the Bellman optimality principle ([6]). The formulation of the optimal control problem for the above system, such that dynamic programming may be used for its solution, has been detailed in Zimmerman, et al. [5]. The following section analyzes those results from the perspective of deriving an implementable rule-based strategy that would replicate the optimal control inputs and trajectory.

3.3. Results and Analysis

For the purpose of dynamic programming, measured parameters obtained for twenty working cycles (~ 197 seconds in total) were used as inputs. Each working cycle is typically 9 to 10 seconds long. For this paper, the interval from t = 108s to 117.2s is studied (**Figure 3**) in more detail. At the starting time, the bucket is fully loaded and at the bottom of the trench. The boom is lifted and the swing rotated toward the truck from t = 108s to t = 110.4 s ('lift and turn'), following which the bucket is emptied ('dump') while the swing is brought to rest (t = 110.4s to t = 111.8s). Next, the swing is returned to trench while the boom is lowered down (t = 111.8s to t = 114.8s). Finally, t = 114.8s to t = 117.2s is the 'dig' phase with use of the stick and bucket.

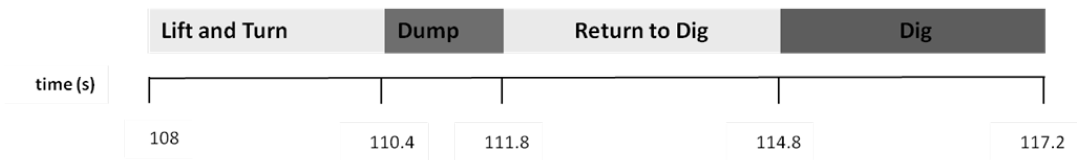

Figure 3: Expert Truck-Loading Cycle

Figure 4 is a plot of actuator velocities, estimated from position measurements. **Figure 5** shows optimal displacements for units 2, 3, 4 and 5.

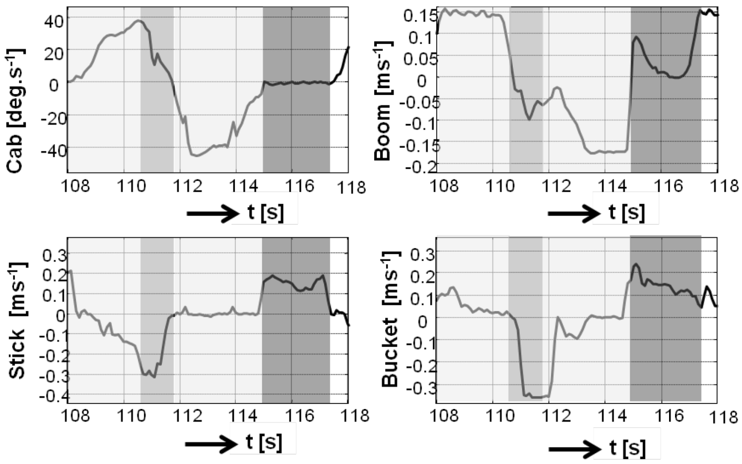

Figure 4: Actuator Velocities

It should be clear that atleast one of the DC pumps (3,4,5: all mechanically linked to the engine shaft) is adjusted to 100% displacement (except from t = 112s to t = 113s). This in turn implies that the engine is at the minimum allowable speed so that the flow requirements may be met at the corresponding actuators in these intervals. The optimal displacement of unit 2 is adjusted to meet the required torque at the swing motor.

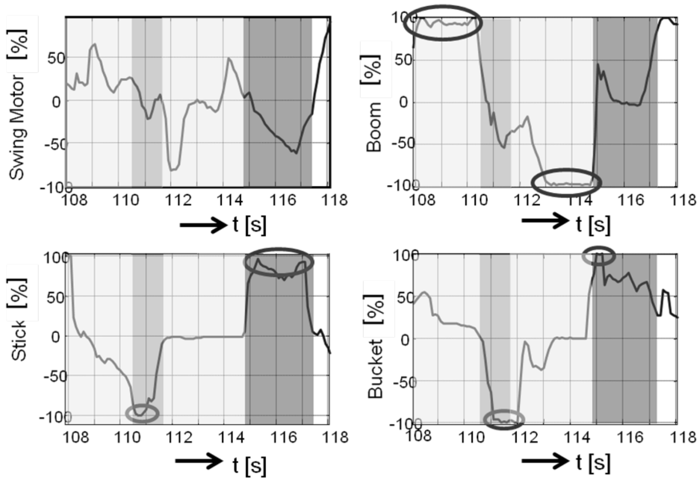

Figure 5: Optimal Pump Displacements

Figure 6 shows the free control variables, u_{thr} and β_1, during the cycle. Except for the interval t = 112s to 113s, the engine throttle is high (90 to 100%), implying that the engine operates close to its maximum torque (while also being at minimum allowable speed). The storage pump (β_1) acts to keep the engine at the optimal speed (explains oscillations on either side of 0%) and the accumulator at optimal pressure (while the swing motor requirements are also met using flow from/to the accumulator).

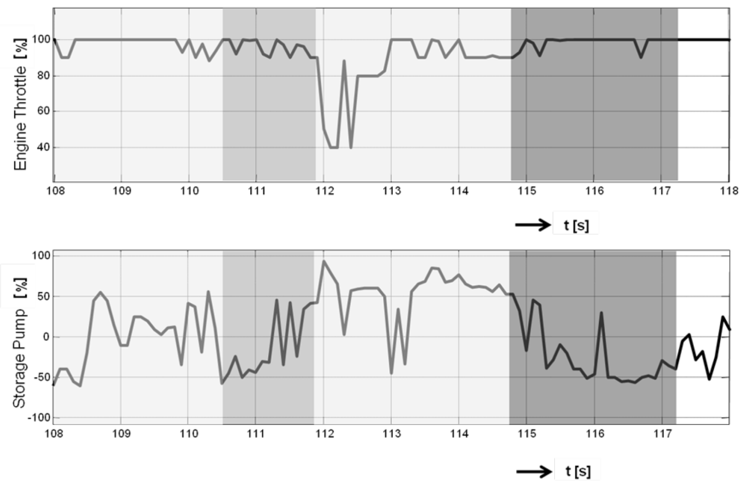

Figure 6: Optimal Engine Throttle (%) and Storage Pump Displacement (%)

For the remainder of this paper, 'Control 1' will refer to the results from optimal control, while 'Control 2' will refer to the proposed rule-based control strategy.

Figures 10 and 11 provide more insight, showing that the accumulator is kept steady at around 280 bar during the lift and dump phase, while being discharged to minimum system pressure while dumping. The accumulator is charged close to relief pressure (350 bar) while returning to trench, taking advantage of the boom being lowered while the swing is brought to rest. Finally, while digging, the accumulator is drained to meet the excess power requirements (Figure 10) on the engine over and above the maximum engine power. For most of the 'dig' phase, the engine speed stays above the minimum engine speed (t = 115.5s to 117.2s), while keeping the stick and bucket pumps at around 70-80%, not 100%.

From t = 112 s to 113s, the engine throttle is lowered while the storage pump is at high displacement, so as to reduce engine speed drastically. Yet, the engine speed is well above the minimum allowable speed, and none of the pumps are close to full displacement.

4. Rule-Based Power Management Strategy

It is instructive to look at cycle power requirements and optimal power outputs before formulating rules. The engine power output, P_{eng}, is mostly high (Fig. 7, recall that maximum engine power is 20.5 kW) during the cycle, except from t = 112s to 113s. This exception occurs in the interval when the DC power requirement P_{DC} (sum of the power requirements of linear actuators) is negative while there is a positive power requirement, P_{sw}, at the swing motor (the swing is being accelerated).

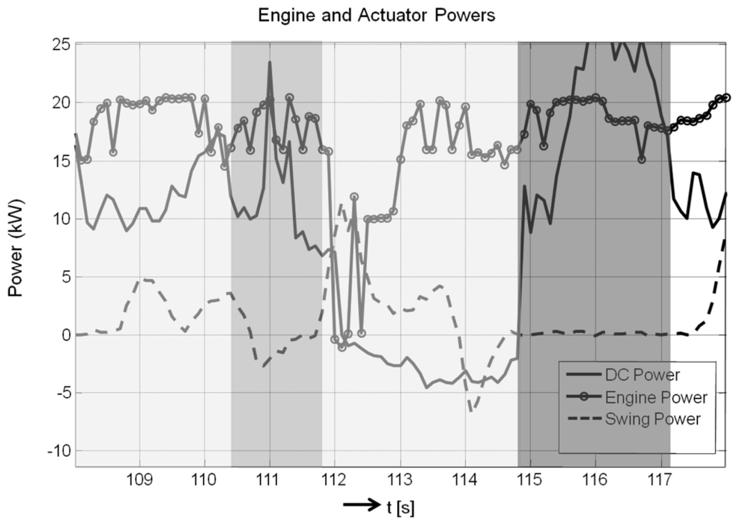

Figure 7: Engine and Actuator Powers (kW)

From t = 113s to t = 114.8 s, the DC power requirement remains negative, while the swing power varies from zero to negative toward the end of this period (swing being brought to rest). In the rest of the cycle, $P_{DC} > 0$ and P_{eng} is kept high (between 15 kW to 20 kW) through a high throttle.

4.1. Rules

The proposed control strategy to replicate optimal control is summarized in **Table 1**, with different rules for different states created using conditions on P_{DC}, the required DC power. Control 1' will refer to enFirstly, the minimum, $n_{CE,min}$ engine speed is pre-computed according to the DC pump flow requirements (Eq.4), assuming each DC pump is at 100%.The calculation of $n_{CE,min}$ is shown in /8/ for a parallel hybrid, but is modified for the series parallel hybrid by only considering the DC pump flow requirements.

$$n_{\mathrm{CE,min}} = \min\left\{ abs\left[\frac{Q_i}{0.95 V_{d,i}}\right], i = 3,4,5 \right\} \tag{4}$$

Table 1		
I. $P_{DC} < 0$	***II. $P_{CE,max} \geq P_{DC} \geq 0$***	***III. $P_{CE,max} < P_{DC}$***
$P_{CE} = min\{P_{ref}, M_1\, \omega_{CE} + P_{req}\}$	$P_{CE} = P_{ref}$	$P_{CE} = P_{CE,max}$
$n_{CE} = n_{CE,min}$	$n_{CE} = n_{CE,min}$	$n_{CE} = n_{CE,min}$
$M_1 = M_{1,max}$	$M_1 = (P_{CE} - P_{req})/\omega_{eng}$	$M_1 = (P_{CE} - P_{req})/\omega_{eng}$

Table 1: Engine Torque and Storage Pump Commands

$$u_{\mathrm{CE}}(\%) = \left(\frac{M_{CE}(\omega_{CE})}{M_{WOT}(\omega_{CE})}\right) \times 100 \tag{5}$$

In states *II* and *III*, the engine is respectively kept at the reference power (P_{ref} = 14.6 kW) and the maximum available power ($P_{CE,max}(n_{CE})$). In state *I*, the engine is operated at the lower among the reference power (P_{ref}) or the power required at the actuators, while keeping the storage pump at 100%, i.e. ($M_{1,max}\, \omega_{CE} + P_{req}$).

The minimum speed command $n_{\mathrm{CE,min}}$ is set to be higher than 1700 rpm at all points of time. This enables operation of the engine at the reference power or higher, if required, and also ensures operation of the engine in largely efficient areas.

The engine throttle command u_{CE} is found from Eq. 5, once the desired engine torque M_{CE} is computed (M_{CE} = P_{CE}/ω_{CE}). The storage pump torque is then determined depending on the state, and the term P_{req} which is computed as follows:

$$P_{\mathrm{req}} = \left(M_{DC} + \frac{J_{CE}(\omega_{CE,\min}(k) - \omega(k-1))}{T_s} \right) \omega_{CE}(k) \tag{6}$$

Typically the term P_{req} is close to P_{DC}, if a small enough sample time, T_s is used. Here T_s = 0.02 seconds in simulation.

In each of these states, there are 'exit states' for the storage pump, so that if the accumulator is empty (at minimum system pressure) or full (at relief pressure), it should be ensured that the accumulator is necessarily only charged ($M_1 \geq 0$) or only discharged ($M_1 \leq 0$), respectively, by the storage pump (these are not shown in Tables 1 and 2). Determination of β_1 from the desired pump torque M_1 is done using an iterative technique (/8/, /5/) that minimizes the error between the desired torque and output torque at a given iteration.

$$\beta_{1(\%)} = f(M_{1,req}, n_1, \Delta p_1) \tag{7}$$

Further, 'anti-stall control' logic is used to prevent the engine from stalling in the extreme case of excessive load at low speeds. For this, the pump commands are proportionally reduced if the engine falls below a certain limit (/9/). For the series-parallel hybrid a limit of 1700 rpm was used.

The fuel rate $\dot{m}_{fuel}(k)$ is determined from the engine brake specific fuel-map (**Figure 16**), whereas the accumulator pressure and engine speed at the next instant is determined by the discretized version of the state model (Eq. (1) and (2)).

4.2. Swing Motor and DC Pump Commands

The required torque from the swing motor, M_2 (together with n_2 and Δp_2) is used to compute β_2 using the same procedures.

$$\beta_{2(\%)} = f(M_{2,req}, n_2, \Delta p_2) \tag{10}$$

The DC pump commands are generated based on the corresponding flow requirements (Q_{req}) with the above iterative procedure extended for this calculation as well.

$$\beta_{i(\%)} = g(Q_{i,req}, n_i, \Delta p_i), \quad i = 3,4,5 \tag{11}$$

4.3. Co-simulation Model

Thus far the rules for generating pump and engine commands have been described. These are part of the 'Controller' of the dynamic co-simulation model (/4/) in **Figure 8**, that includes both the equation of motion and the hydraulics of the excavator system as well as engine dynamics.

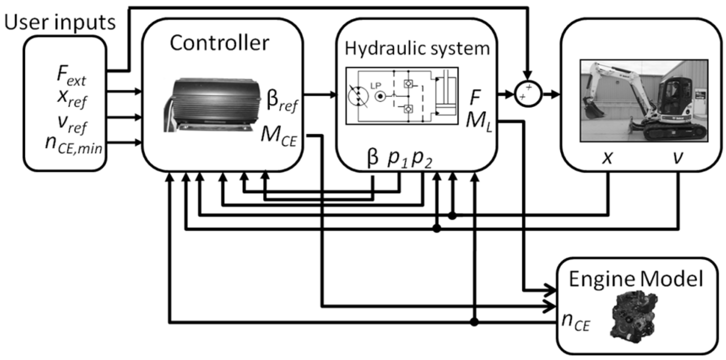

Figure 8: Simulation Model Structure

The pump control system and engine control are not shown explicitly here, and more details on these are given in /8/.

4.4. Results and Discussion

The pump displacements resulting from the proposed rule-based strategy (**Figure 9**) replicate the optimal trends, and it is apparent that atleast one of the DC pumps is at 100%, except in the time period t = 112s to t = 113s. This also means that the minimum engine speed command is being followed in these intervals. In the exceptional interval of t = 112s to t = 113s, the minimum required speed is around 500 rpm (due to low flow requirements from the DC pumps). Since the engine speed commands are saturated to be above 1700 rpm, as mentioned above, the strategy follows optimal trends reasonably well in the above interval too (**Figure 11**).

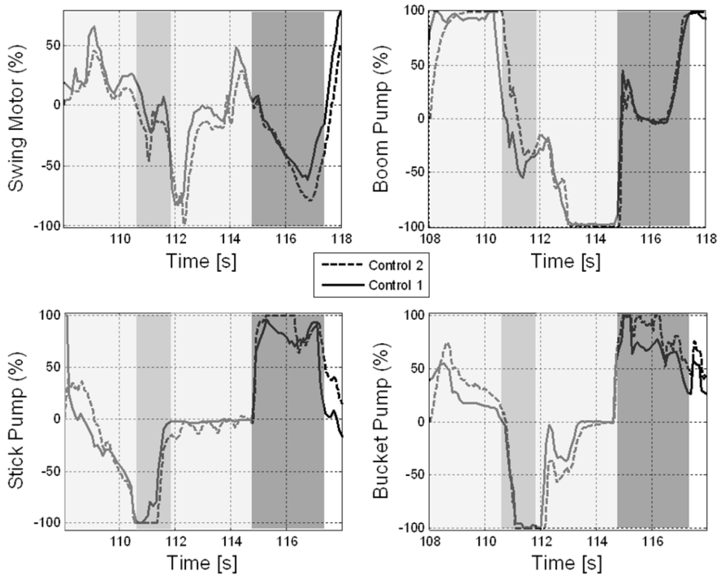

Figure 9: Pump Displacements (%)

The accumulator pressure follows a similar trend as the optimal pressure, except during the early part of the 'lift and turn' phase, wherein the engine power P_{ref} is higher than P_{DC} which leads to the accumulator being charged with the excess available power. Since the storage pump is at +100% displacement in the 'return-to-dig' phase, the accumulator charges faster than in the optimal case.

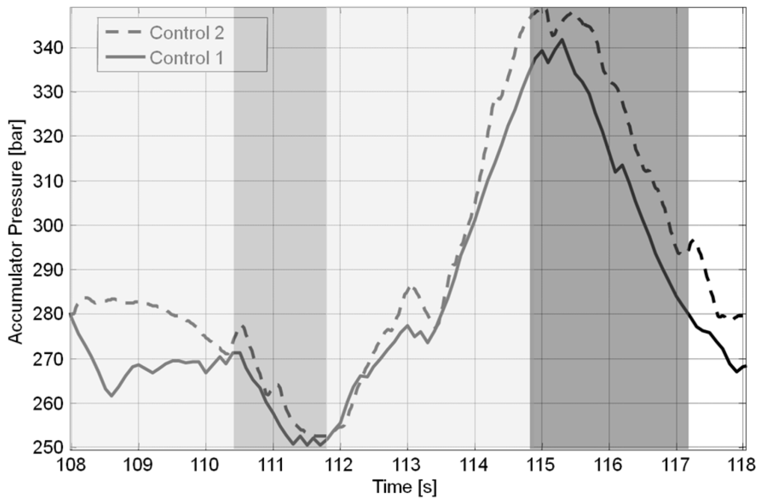

Fig. 10 – High Pressure Accumulator

Figure 11 shows that the simulated engine speed n_{CE} ('Control 2') is lower than the optimal speed ('Control 1'), as would be expected from the rules, during most part of the 'dig' phase. It is lower than the optimal speed during most of the 'lift and dump' phase, which is unexpected.

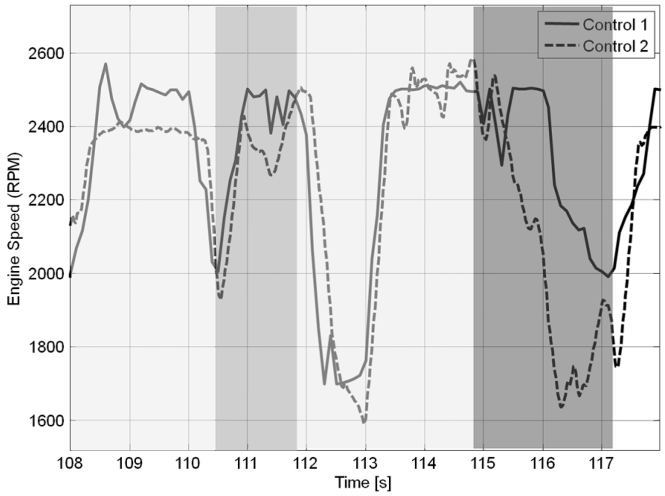

Fig. 11 – Engine Speed

For a simulation period of 27.2 seconds of the working cycle of the machine (t = 98.9s to t = 125.1s), the DC non-hybrid consumed 42 grams /5/. In contrast, the hybrid consumed 33.8 grams with optimal control, and 34.5 grams using the proposed, implementable rule-based control strategy. Hence the series-parallel hybrid can show improvements of upto 17.9% over the DC system, using the proposed control strategy.

It should be noted that the fuel results from the proposed control strategy and those from optimal control have been obtained using dynamic system models with different levels of detail. The dynamic model used for simulation of the proposed control strategy contains accurate, high-fidelity component models, including impedance models for the lines. The state-space model used for the dynamic programming study /5/, had to be a simplified one, because of the computational expense involved.

4.5. Implementation

The rule-based strategy outlined has not been implemented yet, but this will be done following modification of the prototype DC excavator to a hybrid DC excavator. The strategy requires estimation of various quantities – speeds ($n_{CE,min}$), flows ($Q_{req,i}$), loads (M_{DC}, M_{sw}) and powers (P_{DC}, P_{sw}). This can be done online, using the various measured signals on the prototype DC machine, such as pump displacements (β_i), engine (n_{CE}) and swing motor speeds (n_i), pump ($p_{i,j}$) and accumulator pressures (p_{hp}).

5. Conclusions

Optimal control results for the series-parallel hybrid DC excavator were analyzed with the aim of replicating these through an implementable, rule-based strategy. The optimal control results show that atleast one of the DC pumps is kept at 100% at most times during the cycle, implying that the engine speed is at the minimum allowable speed at these times. Additionally the engine throttle is high, which ensures efficient engine operation. The storage pump ensures that the accumulator is charged using excess engine power and discharged when actuator power requirement is above the engine power.

The rule-based control strategy derived from these observations led to reasonably good replication of trends in control histories and state trajectories. This was achieved by ensuring that the engine is commanded to be at minimum allowable speed, and at a high reference power for most part of the cycle.

The implementable control strategy proposed also leads to faster charging of the accumulator as compared to the optimal results, since the engine is set at a reference power that is higher than the average optimal power during the 'lift and dump' part of the cycle. The proposed strategy also maintains the engine at a lower speed than the optimal speed during the 'dig' phase. In the future it is intended to improve these aspects of the rule-based control.

Work will also be undertaken to test such a rule-based strategy on a novice truck-loading cycle, as well as a trench digging cycle. It is also intended to investigate strategies that account for the variation of loads during a cycle, while coming as close as possible to the optimal results.

6. References

/1/ Rahmfeld, R. and Ivantysynova, M. 1998. "Energy Saving Hydraulic Actuators for Mobile Machines." *1st Bratislavian Fluid Power Symposium*, Casta Pila, Slovakia, pp. 47-57.

/2/ Zimmerman, J., Busquets, E. and Ivantysynova, M. 2011. "40% Fuel Savings by Displacement Control Leads to Lower Working Temperatures – A Simulation Study and Measurements." *Proceedings of the 52nd National Conference on Fluid Power*, Las Vegas, Nevada, USA.

/3/ Pettersson, K. and Tikkanen, S. 2009. "Secondary Control in Construction Machinery – Design and Evaluation of an Excavator Swing Drive." *The 11th Scandinavian International Conference on Fluid Power, SICFP'09*, Linköping, Sweden.

/4/ Zimmerman, J. and Ivantysynova, M. 2011. "Hybrid Displacement Controlled Multi-Actuator Hydraulic Systems." *The 12th Scandinavian International*

$M_{s,i}$

Conference on Fluid Power, May 18-20, 2011, Tampere, Finland.

/5/ Zimmerman, J., Hippalgaonkar, R. and Ivantysynova, M. 2011. “Optimal Control for the Series-Parallel Displacement Controlled Hydraulic Hybrid Excavator.” *2011 ASME Dynamic Systems and Control Conference and Bath/ASME Symposium on Fluid Power and Motion Control, Oct. 31- Nov. 2, 2011,* Arlington, VA, USA.

/6/ Kirk, D. E. 2004. *Optimal Control Theory: an Introduction*. Dover Publications, Mineola, New York.

/7/ Heywood, J. 1988. *Internal Combustion Engine Fundamentals*. McGraw-Hill Book Company, Ney York.

/8/ Hippalgaonkar, R., Zimmerman, J. and Ivantysynova, M. 2011. “Investigation of Power Management Strategies for a Multi-Actuator Hydraulic Hybrid Machine System.” *2011 SAE Commercial Vehicle Engineering Congress, Sept. 13 - 14, 2011,* Rosemont, IL, USA.

/9/ Williamson, C. 2010. *Power Management for Multi-Actuator Mobile Machines with Displacement Controlled Hydraulic Actuators*. PhD Thesis, Dept. of Agricultural and Biological Engineering, Purdue University, West Lafayette, IN, USA.

/10/ Chong, E. K.-P., Zak, S. H. 2001. “An Introduction To Optimization.” Second Edition, Wiley Inter-Sciences Series Publications.

7. Nomenclature

β_i	% displacement of i^{th} pump $\{i = 1,2, \ldots, 5\}$	%
$p_{i,j}$	pressure at j^{th} port ($j = 1$ *or* 2) of i^{th} pump	Pa
ω_i	angular speed of rotation of i^{th} pump	rad/s
u_{CE}	% throttle of combustion engine	%
$n_{CE,min}$	minimum allowable engine speed	rpm
n_{CE}	simulated engine speed	rpm
$Q_{s,i}$	Volumetric losses of i^{th} pump	m^3s^{-1}
$M_{s,i}$	Torque losses of i^{th} pump	N.m

M_{DC}	Sum of torques of DC pumps	N.m
V_0	Pre-charge volume of the accumulator	m^3
p_0	Pre-charge pressure of the accumulator	Pa
n	isotropic co-efficient of gas in accumulator	[ ]
V_i	Displacement of the i^{th} pump	m^3/rev
p_{hp}	Pressure of (high pressure) accumulator	Pa

8. Acknowledgement

This research was supported by the Center for Compact and Efficient Fluid Power, a National Science Foundation (NSF, USA) Engineering Research Center (ERC) funded under cooperative agreement number EEC-0540834.